doi.org/10.36721/PJPS.2026.39.10.282.1

Dynamic evolution, prediction and patient stratification of chemotherapy-induced neutropenia in a predominantly breast cancer cohort: A decision-support study for building a bundle care strategy

Shuhui Dai[1#], Xuanhe Zhang[2#], Zhen Qiao[2], Liudan Li[2] and Litong Ye[3]*

[1]Department of Nursing, Zhuhai Center for Maternal and Child Health Care (Zhuhai Women and Children's Hospital), Zhuhai 519000, China

[2]Department of Breast Surgery, Zhuhai Center for Maternal and Child Health Care (Zhuhai Women and Children's Hospital), Zhuhai 519000, China

[3]Hospital Infection Control Department, Zhuhai Center for Maternal and Child Health Care (Zhuhai Women and Children's Hospital), Zhuhai 519000, China

Abstract: **Background**: Chemotherapy-induced neutropenia (CIN) is a common dose-limiting toxicity in patients with solid tumors, often leading to infections, treatment delays, or dose reductions. However, studies on the dynamic patterns of CIN across multiple chemotherapy cycles and their prediction remain limited. **Objectives**: To longitudinally observe CIN evolution across two consecutive cycles, develop a predictive model for severe CIN in cycle 2 (T2) based on cycle 1 (T1) characteristics, and classify patients by early recovery capacity to form a personalized bundle care strategy. **Methods**: This single-center retrospective cohort study using electronic medical record (EMR) data enrolled 138 patients with solid tumors (89.1% breast cancer) who received ≥2 chemotherapy cycles between January 1, 2015, and January 31, 2025, at Zhuhai Maternal and Child Health Care Hospital, China. Neutrophil kinetic parameters were collected for T1 and T2. A multivariable logistic regression model predicted grade 3–4 CIN in T2 using T1 variables, with internal bootstrap validation. K-means clustering based on T1 recovery patterns identified patient subgroups. **Results**: Severe CIN incidence decreased from 88.0% in T1 to 42.7% in T2 ($p<0.001$); neutrophil nadir rebounded from 0.40×10^9/L (IQR: 0.10–0.70) in cycle 1 to 1.05×10^9/L (IQR: 0.50–1.80) in cycle 2 ($p<0.001$). The prediction model (age, T1 nadir, T1 days to nadir, T1 recovery duration) achieved a test AUC of 0.677 and an accuracy of 78.6%. Out of the 138 total patients, 120 with complete recovery data were utilized for clustering analysis, identifying three groups: rapid (n=21), similar (n=79) and slow (n=20). The slow-recovery group exhibited significantly higher rates of febrile neutropenia (25.0% vs. 10.1% and 4.8%, p=0.043) and chemotherapy delays (35.0% vs. 15.2% and 9.5%, p=0.021). **Conclusion**: CIN severity generally improves from first to second cycle, but with substantial inter-individual heterogeneity. A T1-based prediction model combined with recovery stratification can identify high-risk patients for personalized CIN management. Further validation in diverse populations is warranted.

Keywords: Bone marrow recovery capacity; Chemotherapy-induced neutropenia; Dynamic prediction model; Multiple solid tumors; Patient stratification management

Submitted on 20-01-2026 – Revised on 07-03-2026 – Accepted on 31-03-2026

INTRODUCTION

Gynecologic and breast malignancies are among the most common cancers affecting women worldwide and pose a serious threat to women's health and survival (Zhang *et al*., 2025; ElKasar *et al*., 2024; Ashariati *et al*., 2022). Among these, invasive ductal carcinoma (IDC) is the predominant histological subtype of breast cancer, accounting for approximately 70–80% of cases (Liao and Cao, 2023). This study, however, extends its focus to a broader spectrum of gynecologic and breast solid tumors (including IDC, gestational trophoblastic neoplasia and endometrial carcinoma) to investigate a common treatment-related toxicity (Sohrabi *et al*., 2024). Chemotherapy plays a central role in their comprehensive management and has significantly improved outcomes (Hosseini *et al*., 2024). However, chemotherapy-induced myelosuppression—particularly chemotherapy-induced neutropenia (CIN)—remains a common dose-limiting toxicity in clinical practice (Ashariati *et al*., 2022; Bai *et al*., 2026). CIN not only restricts the administered dose intensity and timely delivery of chemotherapy but is also directly associated with increased risks of infection, treatment interruptions and compromised long-term outcomes (Castellanos *et al*., 2024; Castellanos *et al*., 2023; Fujii *et al*., 2025).

The clinical impact of CIN is profound; it is a major precipitant of febrile neutropenia (FN) and severe infections and frequently leads to chemotherapy delays or dose reductions, thereby potentially compromising the completeness of tumor control (Gaumond *et al*., 2025; Hobbs *et al*., 2023). Current guidelines from the American Society of Clinical Oncology (ASCO) (Gyawali *et al*., 2026), the National Comprehensive Cancer Network (NCCN) (NCCN Guidelines®: Hematopoietic Growth Factors, Version 3.2026), and the Infectious Diseases Working Party of the German Society of Hematology and

**Corresponding author:* e-mail: yelitong1@163.com

#These authors contributed equally and are the co-first authors.

Medical Oncology (AGIHO) (Sandherr *et al.,* 2026) recommend primary prophylaxis with G-CSF for patients at high risk of febrile neutropenia (≥20%). Although prophylactic and therapeutic use of granulocyte colony-stimulating factor (G-CSF) has become a standard strategy for managing CIN and has partially reduced the incidence of FN, a substantial proportion of patients still experience recurrent and severe CIN episodes (Huo *et al*., 2023). This highlights the limitations of current management approaches and underscores the need for further optimization of personalized prevention and monitoring strategies (Hutajulu *et al*., 2023; Joseph *et al*., 2023).

Currently, most studies on chemotherapy-induced neutropenia (CIN) focus on identifying risk factors, developing risk prediction models and establishing primary prophylaxis strategies for the first chemotherapy cycle (Kang *et al*., 2024; Li *et al*., 2023; Liao and Cao, 2023). While these studies provide valuable insights for managing isolated CIN events, they fail to fully capture the dynamic nature and heterogeneity of CIN across multiple chemotherapy cycles in real-world clinical settings (Morecroft *et al*., 2024). In practice, patients typically receive multiple consecutive cycles of chemotherapy and bone marrow function may exhibit diverse response trajectories—such as cumulative suppression, adaptation, or progressive deterioration—in response to repeated chemotherapeutic insults (Nasir *et al*., 2022). Although a few recent studies have begun to examine CIN evolution across cycles, they largely remain descriptive, lacking mechanistic exploration and quantitative modeling of these dynamic patterns. Moreover, practical predictive tools capable of providing early warning of CIN risk in subsequent cycles have yet to be established (Ong *et al*., 2022).

In recent years, advances in healthcare informatics and artificial intelligence have enabled longitudinal analysis of real-world electronic health records (EHR) and the application of machine learning models, offering novel methodological support for deepening understanding of dynamic disease processes and enabling precise risk stratification (Payton *et al*., 2024). However, in the field of CIN research, dynamic prediction models that explicitly account for its "recurrent event" nature remain absent (Salako *et al*., 2021). Meanwhile, an emerging strategy to enhance the precision of supportive care involves early phenotypic classification of patients based on dynamic features of bone marrow recovery, followed by risk-stratified management and personalized interventions (Sun *et al*., 2022).

To address these research gaps, a discrete-time longitudinal cohort analysis was designed to systematically track the dynamic evolution of CIN across two consecutive chemotherapy cycles in patients with multiple solid tumors. This study aims to achieve three primary objectives: First, to characterize inter-cycle changes and inter-individual heterogeneity in CIN severity and temporal kinetic parameters; Second, to develop a predictive model for severe (grade 3–4) CIN in the second cycle (T2) based on clinical and neutrophil kinetic features from the first cycle (T1);Third, to apply unsupervised clustering methods to identify patient subgroups with distinct bone marrow response phenotypes, using early neutrophil recovery patterns observed in T1.

These analyses will provide the empirical evidence and decision-support tools necessary to inform and operationalize a bundle care strategy for CIN, enabling prospective risk stratification and personalized interventions in clinical practice.

MATERIALS AND METHODS

Study design

This study is a single-center, retrospective discrete-time cohort study designed to longitudinally observe the dynamic evolution of recurrent chemotherapy-induced neutropenia (CIN) events in a predominantly breast cancer cohort across two consecutive, fixed chemotherapy cycles. The study focuses on two well-defined time points: T1 (the initial chemotherapy cycle) and T2 (the subsequent consecutive cycle). This design enables the characterization of longitudinal changes in CIN and the use of exposure characteristics from the T1 cycle to predict outcomes in the T2 cycle.

Study population

Study cohort and definition of time points

This study identified patients with solid tumors (predominantly breast cancer) who received neoadjuvant or adjuvant chemotherapy between January 1, 2015 and January 31, 2025, from the electronic medical record system of Zhuhai Maternal and Child Health Care Hospital. The T1 time point was defined as the patient's first chemotherapy cycle and the T2 time point was defined as the immediately subsequent consecutive chemotherapy cycle. Selecting two adjacent cycles was intended to minimize potential confounding effects from disease progression or major changes in treatment regimens, thereby focusing specifically on the impact of repeated chemotherapy exposure on neutrophil dynamics (Supplementary Fig. S1).

Inclusion criteria: Pathologically confirmed diagnosis of multiple solid tumors; Age ≥ 12 years; Receipt of at least two cycles of chemotherapy (regimens including anthracyclines, taxanes, or other standard therapeutic protocols); Availability of complete blood count monitoring records; and Availability of comprehensive clinical data, including at a minimum age, sex, tumor stage and specific treatment regimen.

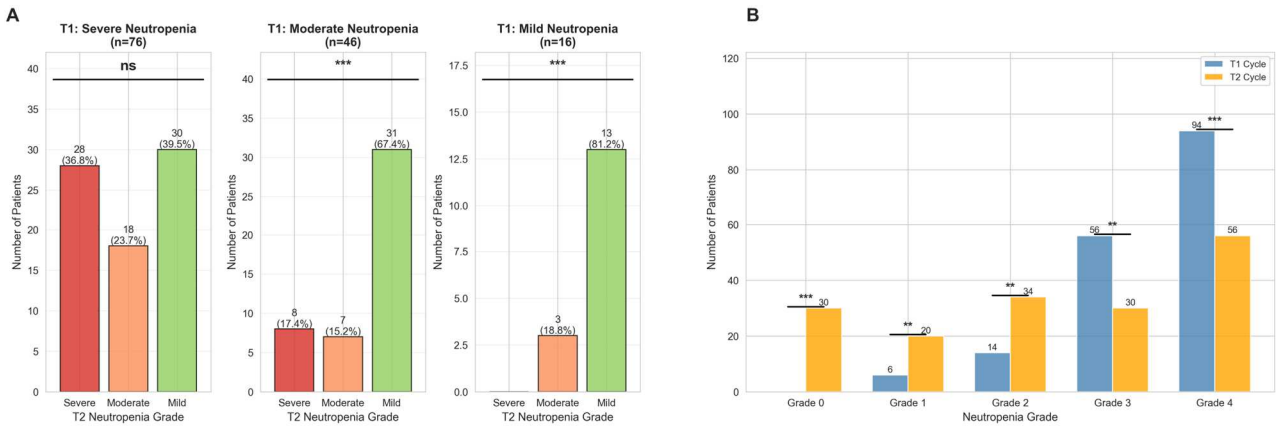

Fig. 1: Neutrophil dynamics across cycles
(A) Stacked bar charts showing the distribution of T2 severity (Mild, Moderate, Severe) stratified by T1 severity. Numbers and percentages of patients are displayed within each bar. Above each subplot, asterisks indicate the result of a chi-square goodness of fit test for equal distribution across T2 categories: Severe group, not significant ($p = 0.196$); Moderate group, $p < 0.001$; Mild group, $p < 0.001$; (B) Paired bar chart comparing CTCAE grades (0–4) between T1 and T2. Values above bars represent patient counts. Horizontal lines with asterisks above each grade pair denote McNemar's exact test for paired proportion differences: Grade 0, $p < 0.001$; Grade 1, $p = 0.004$; Grade 2, $p = 0.005$; Grade 3, $p = 0.003$; Grade 4, $p < 0.001$. Significance symbols: ** $p < 0.01$, *** $p < 0.001$; ns, not significant.

Exclusion criteria: Presence of an active secondary malignancy; Baseline neutrophil count < 1.5 × 10^9/L prior to chemotherapy initiation or a known pre-existing bone marrow failure disorder; Change in core chemotherapeutic agents between the T1 and T2 cycles (e.g., switching from an anthracycline-based regimen to a taxane-only regimen); Receipt of radiotherapy either before the start of the T1 cycle or during the interval between T1 and T2, as radiation may confound bone marrow function.

Because this retrospective EMR-based cohort required documented data from at least two consecutive chemotherapy cycles, conventional loss to follow-up was minimized through the study design (Supplementary Fig. S1). Missing longitudinal kinetic data were handled using a complete-case approach. Specifically, 18 patients with incomplete recovery-related variables were excluded from the unsupervised clustering analysis only, resulting in a final clustering cohort of 120 patients. All other analyses were conducted using the full eligible cohort (n=138).

Data collection and variable definitions
Data for this study were extracted from the electronic medical record system of Zhuhai Maternal and Child Health Care Hospital. A combination of structured database queries and manual verification was used to systematically collect comprehensive information from patients meeting the inclusion and exclusion criteria. All data were de-identified and two independent researchers performed dual data entry and cross-verification to ensure accuracy and consistency. Due to the retrospective nature, information on chemotherapy dose intensity, G-CSF formulation and timing, comorbidities, nutritional status and inflammatory markers was not consistently available, which may introduce residual confounding.

Outcome variables
Primary outcome: Defined as the occurrence of grade 3 or 4 neutropenia during the T2 cycle. Severity grading was based on the Common Terminology Criteria for Adverse Events (CTCAE) version 5.

Dynamic evolution parameters: The following continuous parameters were collected for both the T1 and T2 cycles to describe the longitudinal trajectory of neutropenia:
Neutrophil nadir: The lowest absolute count recorded via laboratory tests within each cycle, measured in $\times 10^9$/L.
Days to nadir: The number of days from the start of chemotherapy administration in each cycle until the neutrophil count reaches its nadir.
Recovery duration: The number of days required for the neutrophil count to first rise and sustainably reach $\geq 1.5 \times 10^9$/L after reaching the cycle's nadir.
Recovery value: The absolute neutrophil count at the time point corresponding to "Recovery Duration," measured in $\times 10^9$/L (operationally defined as the first day when ANC reached $\geq 1.5 \times 10^9$/L and remained above this threshold for at least two consecutive measurements).

Febrile neutropenia (FN), infection-related hospitalization and chemotherapy delays (≥7 days) during T2 as secondary clinical outcomes were also recorded.

Predictive variables and baseline characteristics
All predictive variables were primarily extracted from patient baseline data and the T1 cycle.
Demographic and baseline characteristics: Including age at diagnosis (years), body mass index (BMI).

Tumor characteristics: Including clinical stage, estrogen receptor status, progesterone receptor status and human epidermal growth factor receptor 2 (HER2) status.
Treatment characteristics in T1 cycle: Including specific chemotherapy regimens and whether granulocyte colony-stimulating factor (G-CSF) was used for prophylaxis or treatment during this cycle.
Neutropenia kinetic features in T1 cycle: Specifically, the values of the dynamic evolution parameters during the T1 cycle, including T1 neutrophil nadir, days to nadir in T1 and recovery duration in T1, which are core predictors for model building.
Baseline laboratory indicators: The most recent absolute neutrophil count before the start of chemotherapy.

Derived variables
To facilitate deeper analysis, the following derived metrics were constructed based on original variables:
Recovery Function Categories: Based on the "Recovery Duration" and "Recovery Value" from the T1 cycle, patients were categorized into "rapid recovery," "standard recovery," and "slow recovery" groups through cluster analysis, for subgroup analysis.
Neutropenia evolution patterns: By comparing the severity grading between the T1 and T2 cycles, individual patient trajectories were defined (e.g., "persistent severe," "from severe to mild"), for descriptive analysis purposes.

Sample size calculation
This study aimed to develop a predictive model and perform patient subgroup classification. A sample size estimation was conducted based on the widely accepted "events per variable" (EPV) principle in prediction model research, incorporating the anticipated incidence of grade 3–4 severe neutropenia in the T2 cycle (approximately 35%) and the preliminary set of candidate predictors. Taking this estimation into account—and balancing it against the practical realities of data availability in retrospective real-world studies—a target sample size for the study was established.

After rigorous screening following the protocol outlined in Supplementary Fig. S1, a total of 138 patients m*et a*l inclusion and exclusion criteria and were included in the final analytic cohort to build the predictive model for severe neutropenia in the T2 cycle. For the unsupervised phenotypic clustering analysis, a complete-case approach was adopted; 120 patients possessed the necessary complete kinetic recovery profiles and were utilized for grouping, while 18 patients were excluded solely from the clustering sub-analysis due to missing recovery velocity data points.
To mitigate the risk of overfitting due to limited sample size, the following strategies were implemented:
Parsimonious modeling: Guided by clinical knowledge and univariate analyses, only four key predictors were included—age, T1 neutrophil nadir, days from T1 chemotherapy initiation to nadir and T1 neutrophil recovery duration—in a multivariable logistic regression model.
Internal validation: Model performance was internally validated using 500 bootstrap resampling iterations on the training set (n = 96), yielding confidence intervals for metrics such as the area under the ROC curve (AUC) to ensure robust evaluation.
Data-driven clustering: Patients were stratified into three subgroups via K-means clustering, with the optimal number of clusters determined objectively using the silhouette coefficient and elbow method, ensuring that groupings emerged from intrinsic data structure rather than subjective assumptions.
Robustness checks: Sensitivity analyses were performed by repeating data splits with different random seeds and testing alternative algorithms (e.g., hierarchical clustering) to confirm the consistency and reliability of the findings.

Statistical analysis
All statistical analyses for this study were conducted using R software (version 4.3.0). A two-sided P-value < 0.05 was considered statistically significant.

Descriptive statistics and dynamic evolution analysis
Continuous variables were described as mean ± standard deviation or median (interquartile range) based on their distribution; categorical variables were summarized as frequencies (percentages). For dynamic parameter comparisons, paired data were analyzed to examine longitudinal changes in CIN parameters between the T1 and T2 cycles. Paired t-tests were used for normally distributed continuous variables, while Wilcoxon signed-rank tests were applied for non-normally distributed or ordinal variables (e.g., neutropenia severity grading). Visualization of evolution patterns was achieved through stacked plots to illustrate individual patient trajectories of neutropenia severity across cycles.

Prediction model construction and validation (for severe neutropenia in T2 cycle)
The objective was to develop a model based on T1 cycle characteristics to predict the risk of grade 3–4 severe neutropenia in the T2 cycle. Data from the final cohort of 138 patients were randomly split into a training set (n=96) and a test set (n=42) at approximately a 7:3 ratio for model development and performance evaluation, respectively. Variable selection and model building involved incorporating four key T1 cycle variables—age, T1 neutrophil nadir, days to nadir in T1 and recovery duration in T1—into a multivariable logistic regression framework based on clinical significance and univariate analysis. Model performance was assessed by discrimination (AUC-ROC on the independent test set, with accuracy, sensitivity and specificity reported at the optimal cutoff determined by the Youden index), calibration (calibration curve comparing predicted probabilities with actual outcomes)

and clinical utility (decision curve analysis evaluating net clinical benefit compared to default strategies).

Patient recovery function cluster analysis

The aim was to classify patients based on bone marrow recovery characteristics in the T1 cycle. K-means clustering was performed on standardized "T1 recovery duration" and "T1 recovery value." The optimal number of clusters (K=3) was determined using the elbow method and average silhouette score. Cluster definitions were clinically conceptualized as rapid recovery, similar recovery and slow recovery groups based on cluster centroids. Clinical validation was performed using Kruskal-Wallis H tests to compare T2 cycle outcomes (e.g., T2 neutrophil nadir, T2 recovery duration) among different recovery function groups. K-means was chosen for its simplicity and interpretability with two continuous variables. The optimal number of clusters (k=3) was determined by both the elbow method and average silhouette width. To assess robustness, hierarchical clustering was also performed using Ward's method, which yielded highly similar groupings (adjusted Rand index = 0.89).

Decision tree classification model (for interpretable prediction paths of recovery function)

An intuitive model was developed to predict which recovery function category a patient belongs to, using classification decision tree algorithms with "T1 recovery duration" and other variables as splitting nodes.

Sensitivity analysis

To ensure the robustness of main findings, sensitivity analyses included:

Model stability analysis: Repeating train/test splits with three different random seeds and retraining logistic regression models.

Cluster method stability analysis: Performing hierarchical clustering (Ward's method) on the same variables to assess stability of clustering results.

RESULTS

Characteristics of the study cohort

This study ultimately included 138 eligible patients for analysis, all of whom were female and completed at least two consecutive chemotherapy cycles (T1 and T2). The average age of the patients was 49.5 ± 11.2 years, with an age range from 12 to 74 years. Among them, 123 (89.1%) were diagnosed with breast invasive ductal carcinoma, with the remaining 15 (10.9%) comprising other gynecologic malignancies including gestational trophoblastic neoplasia, endometrial carcinoma, ovarian cancer and cervical cancer. In terms of clinical staging, the majority were at stage II (56 patients, 40.6%) and stage III (42 patients, 30.4%). The most commonly used chemotherapy regimen during the first cycle (T1) was AC (52 patients, 37.7%) followed by taxane plus carboplatin (37 patients, 26.8%). The main baseline characteristics and treatment-related data of the T1 cycle are summarized in table 1. Of note, during the first cycle (T1), 54.3% of patients received antibiotics and 34.8% presented with fever, reflecting the high clinical burden of severe neutropenia. These events may have prompted more aggressive supportive measures—such as prophylactic G-CSF use or dose adjustments—in the subsequent T2 cycle, potentially contributing to the observed improvement in neutrophil outcomes.

Dynamic evolution patterns of neutropenia

To longitudinally observe the evolution patterns of CIN, patients' neutrophil kinetic parameters were compared across T1 and T2. Consistently, the neutrophil nadir rebounded markedly from a median of 0.40×10^9/L (IQR: 0.10–0.70) in T1 to a median of 1.05×10^9/L (IQR: 0.50–1.80) in T2 ($p < 0.001$, Fig. 1 and Table 2), indicating an overall trend of alleviated bone marrow suppression in subsequent cycles. The patient-level incidence of severe (grade 3–4) neutropenia decreased from 88.0% in T1 to 42.7% in T2 ($p < 0.001$).

Further analysis of patient-level severity transitions (Supplementary Fig. S2A) revealed substantial inter-individual heterogeneity: among patients with severe neutropenia in T1 (n=76), 39.5% improved to mild, 23.7% to moderate and 36.8% remained severe in T2; among those with moderate neutropenia in T1 (n=46), 67.4% improved to mild, 15.2% remained moderate and 17.4% worsened to severe; and patients with mild neutropenia in T1 (n=16) mostly stayed mild (81.2%), with 18.8% transitioning to moderate and none to severe.

At the measurement level, the proportion of severe neutropenia (grades 3–4) decreased significantly from 87.4 % (132/151 measurements) in T1 to 46.4% (64/138 measurements) in T2 ($p < 0.001$, Supplementary Fig. S2B). This measurement-based proportion is expected to be slightly higher than the patient-level incidence (42.7% in T2) because patients with persistent severe neutropenia contribute multiple measurements. These patterns highlight both the overall improvement and the existence of a subgroup with persistently poor recovery.

Prediction model construction and performance

Model performance and key predictors

The multivariable logistic regression model for predicting severe neutropenia in T2 achieved a test set AUC of 0.677 and accuracy of 78.6% (Table 3). The ROC curves (Fig. 2A) showed training and test AUCs of 0.767 and 0.677, respectively.

Table 1: Patient baseline characteristics

Characteristic	Value
Total Patients	138
Age (years)	
Mean ± SD	49.5 ± 11.2
Range	12 ~ 74
Gender	
Female	138 (100%)
Tumor Type	
Breast Invasive Ductal Carcinoma	123 (89.1%)
Other Types (gestational trophoblastic neoplasia, high-grade serous carcinoma of the ovary, endometrioid adenocarcinoma of the endometrium, etc.)	15 (10.9%)
Clinical Stage (Summarized)	
Stage I	18 (13.0%)
Stage II	56 (40.6%)
Stage III	42 (30.4%)
Stage IV	15 (10.9%)
Missing/Unclear	7 (5.1%)
Main Chemotherapy Regimen in T1	
AC (adriamycin + cyclophosphamide)	52 (37.7%)
Taxane + Carboplatin	37 (26.8%)
Other regimens (e.g., NP, TC, TA, gemcitabine, etc.)	49 (35.5%)
Fever in T1	
Yes	48 (34.8%)
No	81 (58.7%)
Missing	9 (6.5%)
Antibiotic Use in T1	
Used	75 (54.3%)
Not used	56 (40.6%)
Missing	7 (5.1%)

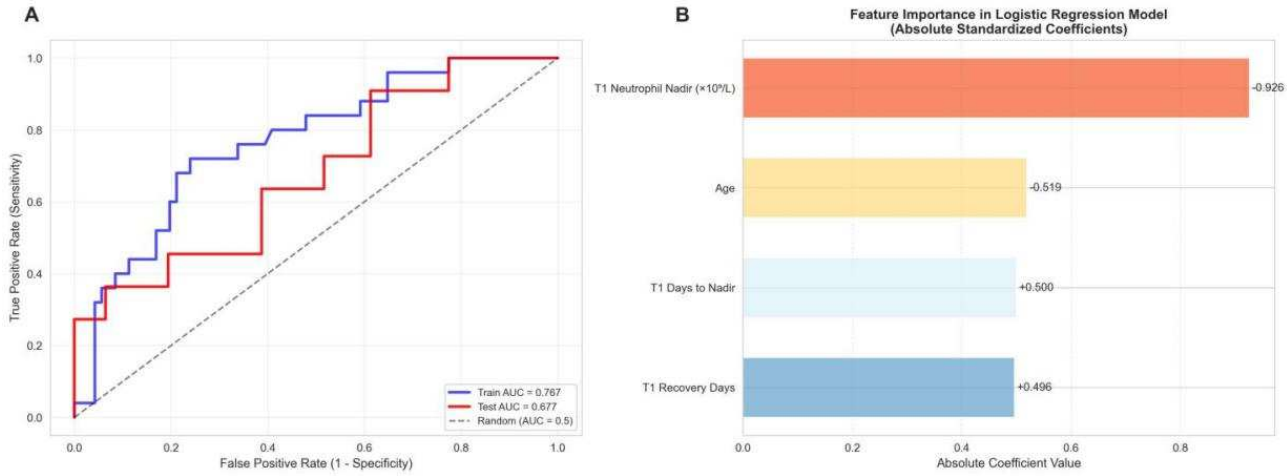

Fig. 2: Predictive model performance
(A) ROC curves of the logistic regression model for predicting severe neutropenia in T2. Training AUC = 0.767, test AUC = 0.677; (B) Feature importance based on absolute standardized coefficients: age (−0.519), T1 nadir (−0.926), T1 days to nadir (0.500), T1 recovery days (0.496).

Table 2: Comparison of neutropenia characteristics between the T1 and T2 cycles

Variables	T1 Median (IQR)	T2 Median (IQR)	Mean difference (95% CI)	Paired t-test p-value	Wilcoxon p-value
Neutrophil nadir (×10⁹/L)	0.40 (0.10–0.70)	1.05 (0.50–1.80)	1.000 (0.730, 1.270)	< 0.001	< 0.001
Days from chemotherapy initiation to nadir (days)	11.00 (9.00–13.00)	10.00 (8.00–15.00)	-0.370 (-1.320, 0.580)	0.571	0.268
Neutrophil recovery duration (days)	3.00 (3.00–5.00)	3.00 (0.00–6.00)	0.060 (-1.090, 1.210)	0.757	0.399
Neutrophil recovery value (×10⁹/L)	4.60 (3.15–8.35)	3.80 (2.70–6.15)	-0.910 (-2.280, 0.460)	0.611	0.059
Neutropenia grade	-	-	-	-	< 0.001

Table 3: Multivariable analysis of the neutropenia recovery prediction model

Intercept	-1.336	0.249	0.263	(0.161, 0.428)	p < 0.001
Age	0.353	0.226	0.703	(0.451, 1.095)	0.119
T1_Neutrophil nadir	-1.178	0.321	0.308	(0.164, 0.578)	p < 0.001
T1_Days from chemotherapy initiation to nadir	0.436	0.244	1.547	(0.960, 2.494)	0.073
T1_Neutrophil recovery duration	0.465	0.240	1.592	(0.994, 2.550)	0.053

Model statistics log-likelihood: -67.40; AIC: 144.81; BIC: 159.44; Pseudo R^2: 0.149, LR p-value: 0.0001
Prediction performance AUC: 0.677; Accuracy: 0.786; Sensitivity: 0.364; Specificity: 0.935;
Optimal Threshold: 0.661; Youden's J: 0.299; Sample Size: 138 (Train: 96, Test: 42)

After bootstrap optimism correction (500 iterations), the optimism-adjusted AUC was 0.653 (95% CI: 0.601–0.705), indicating modest but stable discrimination. Feature importance analysis (Fig. 2B) based on absolute standardized coefficients identified T1 neutrophil nadir (standardized coefficient −0.926), age (−0.519), T1 days to nadir (0.500) and T1 recovery duration (0.496) as key predictors. Decision curve analysis (Fig. 3) demonstrated that the prediction model provided a positive net benefit across clinically relevant threshold probabilities (approximately 20–40%), with a maximum net benefit of 0.254—approaching the theoretical upper bound defined by the event rate (0.262). This indicates that using the model to guide clinical decisions would yield superior outcomes compared to either treating all or treating no patients, supporting its potential utility despite modest discrimination.

Model interpretability and calibration

An intuitive decision tree (Fig. 4) was constructed to classify patients into recovery groups, using T1 recovery duration as the primary splitting node. The test set accuracy was 69.4%. Calibration curves (Fig. 5) demonstrated that logistic regression predictions aligned more closely with observed outcomes than random forest, supporting reliable probability estimates.

Patient recovery function classification and its clinical significance

Of the 138 total patients, 120 had complete data for both T1 recovery duration and T1 recovery value and were included in the clustering analysis. Based on T1 recovery patterns, K-means clustering identified three distinct patient groups: rapid recovery (n=21), similar recovery (n=79) and slow recovery (n=20) (Fig. 6A). Significant heterogeneity among groups was observed in key kinetic parameters (Table 4). For instance, the rapid recovery group had a longer T1 recovery duration but exhibited the highest T2 neutrophil nadir and shortest T2 recovery time, whereas the slow recovery group showed persistently poor recovery (Fig. 6B and Table 4).

Clinical outcomes across recovery groups

The slow-recovery group had a higher incidence of febrile neutropenia (25.0% vs. 10.1% in similar-recovery and 4.8% in rapid-recovery, p=0.043) and more frequent chemotherapy delays (35.0% vs. 15.2% vs. 9.5%, p=0.021). Hospitalization rates showed a similar trend but did not reach statistical significance (p=0.112). These findings support the clinical relevance of the recovery-based stratification (Table 5).

DISCUSSION

Chemotherapy-induced myelosuppression is a common complication in cancer treatment (Wang *et al*., 2023). Its core pathophysiological mechanism lies in the direct cytotoxic effects of chemotherapeutic agents on hematopoietic stem and progenitor cells in the bone marrow—particularly granulocytic precursors—leading to impaired production, disrupted maturation and depletion of the circulating neutrophil pool (Wuerstlein *et al*., 2021; Zhang *et al*., 2024). Neutropenia (CIN) represents the most rapid and frequent manifestation of this process and its severity and duration directly influence infection risk and treatment continuity.

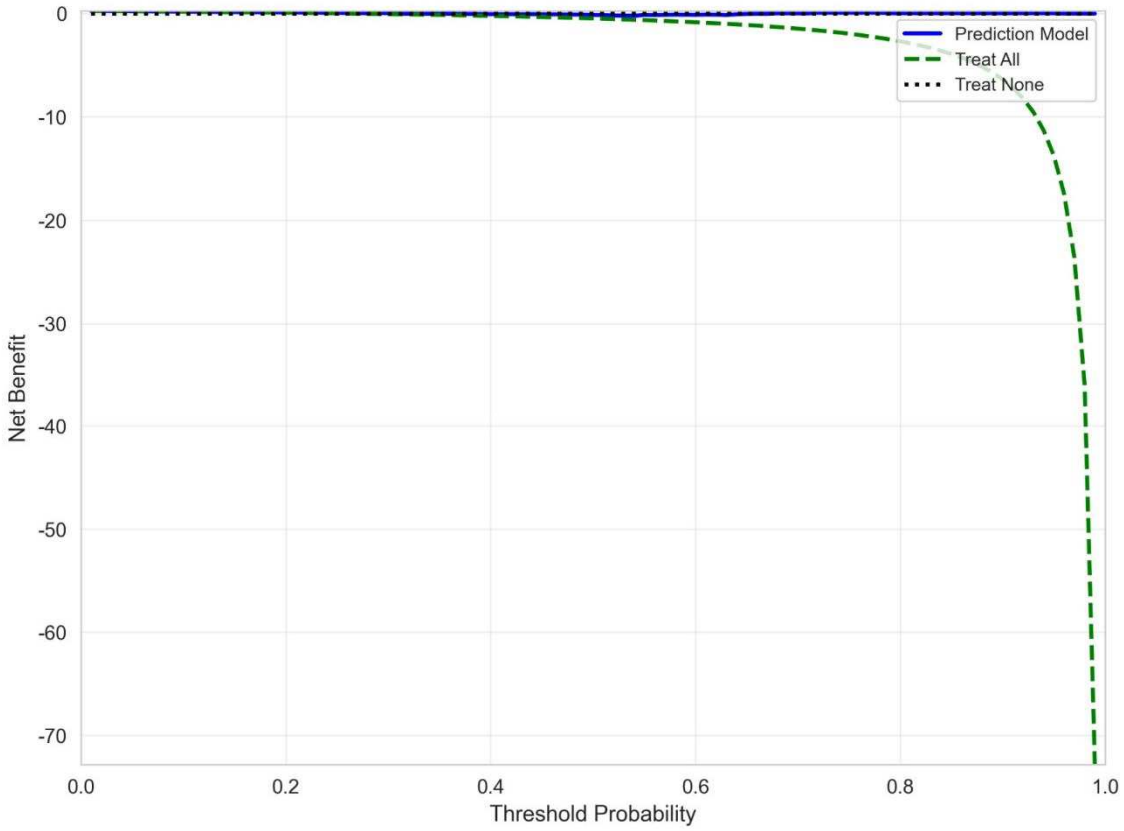

Fig. 3: Decision curve analysis

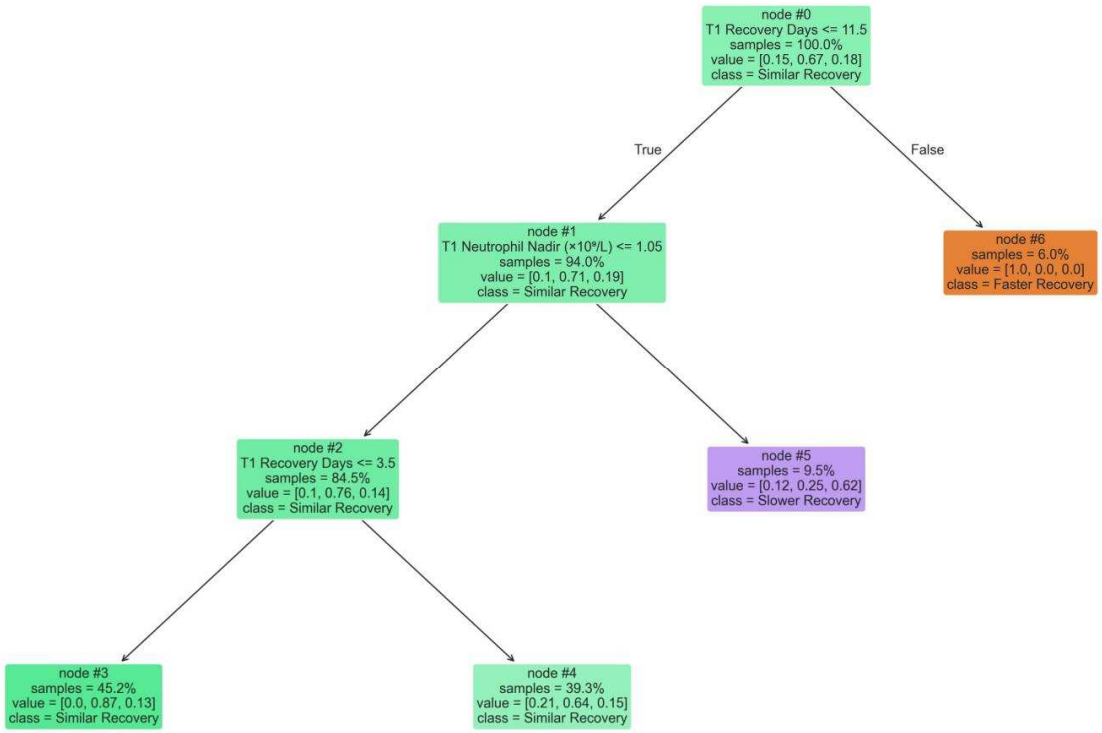

Fig. 4: Decision tree for recovery group classification.

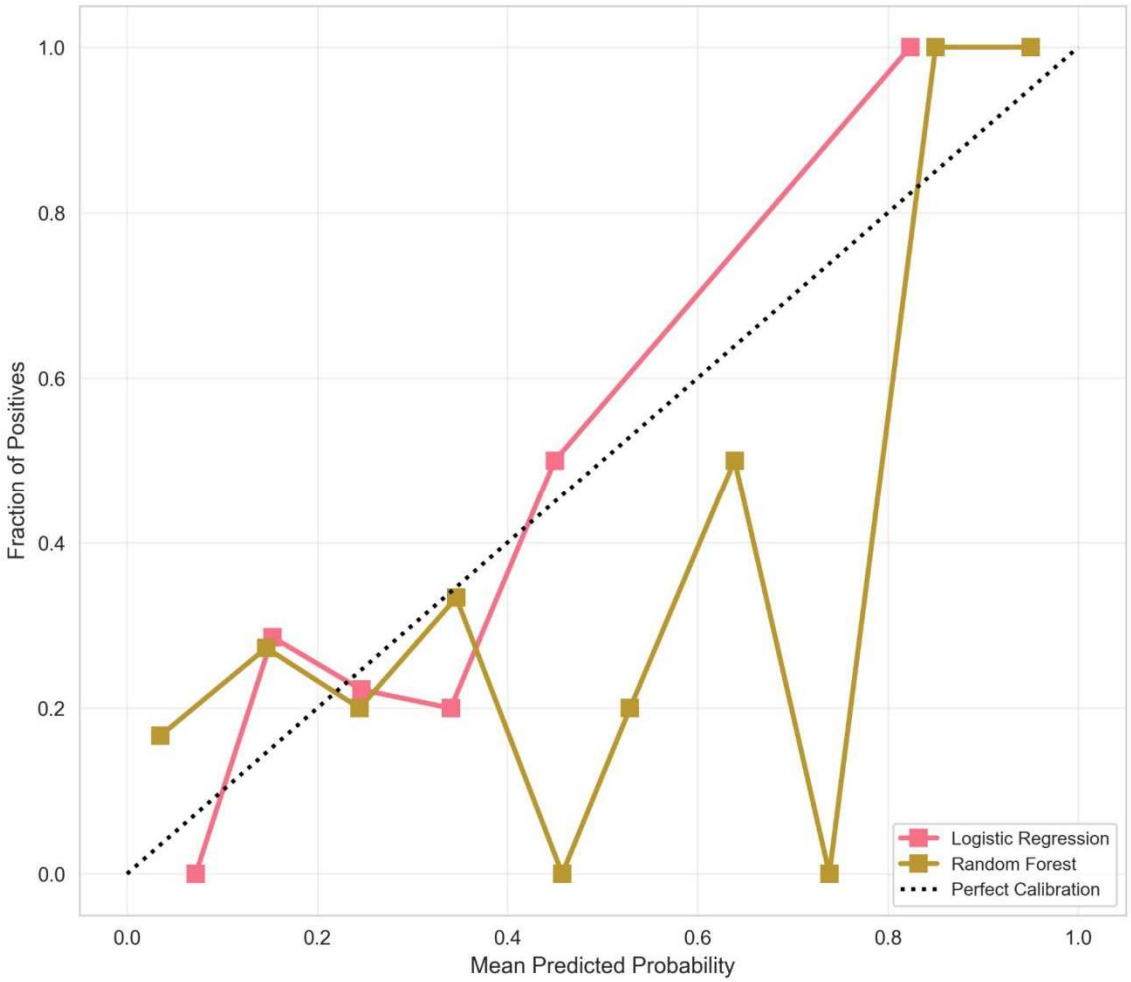

Fig. 5: Calibration curve

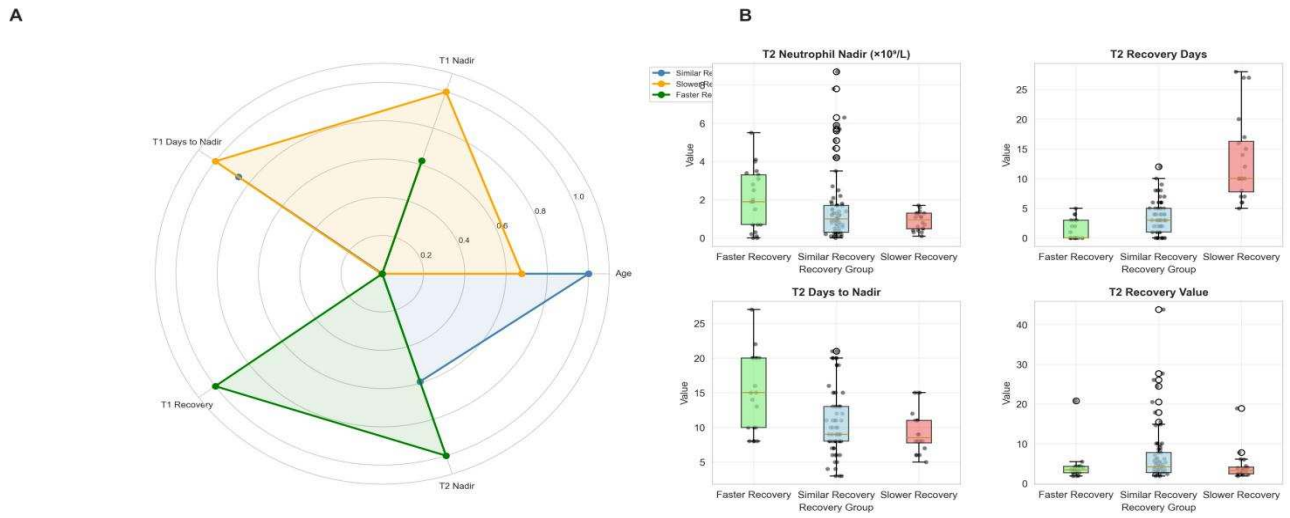

Fig. 6: Patient recovery groups.
(A) Radar chart of normalized mean values for five key variables across recovery groups (Similar: n=79, Slow: n=20, Rapid: n=21); (B) Box plots comparing T2 outcomes: T2 neutrophil nadir (p=0.196), T2 recovery days (p<0.001), T2 days to nadir (p=0.001) and T2 recovery value (p=0.066). p-values from Kruskal-Wallis test.

Table 4: Patient characteristics by neutropenia recovery function classification.

Variables	Similar recovery group (n=79)	Slow recovery group (n=20)	Rapid recovery group (n=21)	F/H	p
Age (years)	48.01±10.37 [48.00(42.00,56.50)]	47.30±13.53 [46.00(41.50,54.50)]	45.81±8.80 [44.00(39.00,51.00)]	0.358	0.701
T1 neutrophil nadir (×10⁹/L)	0.41±0.33 [0.30(0.10,0.65)]	0.61±0.56 [0.35(0.18,0.88)]	0.53±0.41 [0.40(0.30,0.80)]	2.642	0.267
Days from T1 chemotherapy initiation to nadir (days)	12.01±4.21 [12.00(9.50,13.00)]	12.30±5.09 [11.00(9.75,13.50)]	10.24±2.53 [11.00(8.00,12.00)]	3.581	0.169
T1 neutrophil recovery duration (days)	3.53±2.10 [3.00(2.00,4.00)]	3.55±1.36 [3.00(3.00,4.00)]	9.38±4.88 [7.00(5.00,13.00)]	30.511	<0.001**
T2 neutrophil nadir (×10⁹/L)	1.55±1.84 [1.00(0.30,1.70)]	0.89±0.48 [0.95(0.47,1.30)]	2.01±1.61 [1.90(0.70,3.30)]	3.278	0.196
Days from T2 chemotherapy initiation to nadir (days)	10.52±4.78 [9.00(8.00,13.00)]	9.35±3.07 [8.50(7.75,11.00)]	15.20±5.71 [15.00(10.00,20.00)]	13.233	0.001*
T2 neutrophil recovery duration (days)	3.27±2.70 [3.00(1.00,5.00)]	13.25±7.25 [10.00(7.75,16.25)]	1.29±1.71 [0.00(0.00,3.00)]	62.614	<0.001**

Data are mean ± SD (median [IQR]). P-values from ANOVA or Kruskal-Wallis. * P=0.001; ** P<0.001. No symbol = not significant (P⩾0.05).

Table 5: Clinical outcomes across recovery function groups during the T2 cycle

Outcome	Rapid recovery (n=21)	Similar recovery (n=79)	Slow recovery (n=20)	χ^2	p-value
Febrile neutropenia, n (%)	1 (4.8%)	8 (10.1%)	5 (25.0%)	6.312	0.043
Chemotherapy delay (≥7 days), n (%)	2 (9.5%)	12 (15.2%)	7 (35.0%)	7.754	0.021
Infection-related hospitalization, n (%)	1 (4.8%)	6 (7.6%)	4 (20.0%)	4.385	0.112

Note: p-values were calculated using chi-square test or Fisher's exact test as appropriate.

Although the use of granulocyte colony-stimulating factor (G-CSF) has substantially improved CIN management, the heterogeneous responses observed among patients suggest that individual tolerance and recovery patterns in response to repeated chemotherapy are shaped by a complex interplay of factors—including baseline bone marrow reserve, genetic variations in drug metabolism and the bone marrow microenvironment (Zhang Q *et al*., 2024; Zhang Y *et al*., 2024; Zhao *et al*., 2021).

The observed improvement from T1 to T2—reduced CIN severity and higher neutrophil nadirs—is clinically expected given the near-60% rate of grade 4 neutropenia in T1, which would mandate intervention per guidelines. This improvement is likely attributable to increased use of prophylactic G-CSF, dose modifications, or enhanced supportive care in response to severe neutropenia during the first cycle, rather than intrinsic bone marrow adaptation. This interpretation is supported by the high rates of fever (34.8%) and antibiotic use (54.3%) in T1, which may have triggered more aggressive clinical management in T2. However, as G-CSF administration data were not systematically collected, the exact contribution of specific interventions requires quantification in future prospective studies. Although the predictive model achieved only moderate discrimination (test set AUC = 0.677), its calibration and net benefit (maximum 0.254) at clinically relevant thresholds support its potential as a decision aid, particularly when integrated with clinical judgment.

The model utilizes readily accessible early indicators—age, T1 neutrophil nadir and time from T1 chemotherapy initiation to nadir—to estimate risk in subsequent cycles. T1 neutrophil nadir emerged as the strongest independent

predictor, directly reflecting the depth of initial bone marrow suppression and serving as a simple early warning tool.

Through unsupervised clustering based on T1 recovery dynamics, patients were classified into three distinct groups: rapid recovery (n=21), similar recovery (n=79) and slow recovery (n=20). The rapid recovery group, characterized by longer T1 recovery times but the highest T2 neutrophil nadir and shortest T2 recovery duration, may possess stronger bone marrow reserve and repair capacity. In contrast, the slow recovery group exhibited persistent marrow suppression across both cycles, with higher rates of febrile neutropenia (25.0%) and chemotherapy delays (35.0%), marking them as true high-risk individuals requiring intensified monitoring and supportive care. The similar recovery group represents the most common clinical phenotype. This functional stratification introduces a "recovery capacity" dimension to risk assessment, enabling more refined patient management.

By integrating predictive modeling with unsupervised clustering, this study transforms early kinetic features into a dual-purpose tool for risk prediction and functional stratification. The decision tree model provides an intuitive triage pathway and together these tools offer a data-driven framework for implementing risk-adapted, proactive bundle care that can improve patient safety and treatment intensity while optimizing resource utilization.

Nevertheless, this study has several limitations. First, its single-center retrospective design and limited sample size—despite internal validation using bootstrap resampling—constrain the external generalizability of both the predictive model and the recovery-based classification, necessitating validation in large-scale prospective cohorts. Second, the observation of only two consecutive chemotherapy cycles precludes insights into longer-term CIN trajectories across the entire treatment course. Furthermore, potentially important variables, such as pharmacogenomic profiles, cytokine signatures and detailed comorbidity data, were not included. The single-center retrospective design and the predominance of breast cancer patients (89.1%) limit the generalizability of findings to other solid tumors. Future multicenter studies with broader inclusion are warranted. The present analysis was restricted to only two consecutive chemotherapy cycles, which may not capture the full trajectory of CIN over the entire treatment course. Longer-term studies are needed to understand cumulative effects and late recovery patterns. Important confounders such as chemotherapy dose modifications, G-CSF administration details, baseline inflammatory status and performance status were not fully accounted for. Their omission could bias the observed associations and limit causal inference. Although bootstrap resampling was used for internal validation, the lack of independent external validation limits the generalizability and reproducibility of both the prediction model and the clustering results. Prospective multicenter studies are essential to confirm these findings. Fourth, although patients with major changes in core chemotherapeutic agents were excluded, minor dose adjustments or schedule modifications between treatment cycles could not be fully accounted for. Such unmeasured variations may influence neutrophil dynamics and introduce residual confounding.

Looking ahead, future research should focus on conducting multicenter prospective validation studies, integrating multi-omics data (e.g., genomic, immunologic) to develop higher-performance predictive models, extending the observation window to investigate associations between CIN dynamics and long-term survival outcomes and launching interventional trials based on the "recovery function classification" to evaluate whether personalized intensified prevention strategies (e.g., preferential use of long-acting G-CSF or algorithm-guided dose adjustments) for high-risk "slow-recovery" patients can improve clinical outcomes.

CONCLUSION

In summary, this study advances the understanding of recurrent chemotherapy-induced neutropenia (CIN) in a predominantly breast cancer cohort across three dimensions: dynamic evolution, predictive early warning and functional stratification. The developed prediction model and recovery-function classification system provide empirical evidence and a practical framework for clinicians to identify high-risk patients early and implement individualized, proactive CIN management—thereby enhancing patient safety and treatment quality while maintaining therapeutic intensity.

Acknowledgment
ChatGPT 5.2 was used for the purpose of language improvement.

Authors' contributions
Shuhui Dai and Xuanhe Zhang contributed equally to this work and share first authorship. Shuhui Dai was responsible for study conception and design, data collection and curation, and drafting of the initial manuscript. Xuanhe Zhang was responsible for study conception and design, data collection and curation, and drafting of the initial manuscript. Zhen Qiao performed data collection and curation, statistical analysis, and assisted with model development. Liudan Li performed statistical analysis and assisted with model development. Litong Ye supervised the study, provided critical intellectual input, and revised the manuscript for important academic content. All authors contributed to interpretation of the data, critically reviewed the manuscript, approved the final version, and agree to be accountable for all aspects of the work.

Funding
This work was supported by the 2023 Zhuhai Medical Research Project (No.2220009000242) and Zhuhai Science and Technology Plan Project in the Field of Social Development (No.2420004000202).

Data availability statement
The datasets generated and/or analysed during the current study are available from the corresponding author on reasonable request.

Ethical approval
This retrospective study was approved by the Institutional Review Board of Zhuhai Maternal and Child Health Care Hospital (Approval No.2023011606), which granted a waiver of informed consent for the analysis of pre-existing, de-identified medical records collected from January 1, 2015. All procedures involving human participants were in accordance with the Declaration of Helsinki (as revised in 2013). This study was performed in adherence with the RECORD guidelines. See supplementary file for the RECORD checklist.

Conflict of interest
The authors have no conflicts of interest to declare.

Supplementary data
https://www.pjps.pk/uploads/2026/07/SUP1783151327.pdf

REFERENCES

Ashariati A, Bintoro UY, Savitri M, Diansyah MN, Amrita PNA, Romadhon PZ, Wijaya AY, Hendrata WM, Looi SS and Mahmudin AA (2022). Factors associated with absolute neutrophil count dynamics and docetaxel-adryamicin-cyclophosphamide (TAC) chemotherapy induced neutropenia during extended filgrastim administration in breast cancer patients. *Acta Med Indones*, **54**(3): 371-378.

Bai Y, Agustinus AS, Yomtoubian S, Meydan C, McNally DR, Yoffe L, Hubisz MJ, Tranquille M, Pramod S, Hong C, Plasilova ML, Kapoor AR, Singh A, Withers H, Dow LE, Laughney AM, Bhinder B, Elemento O, Melnick AM, Bakhoum SF and Mittal V (2026). Epigenetic regulation of chromosomal instability by EZH2 methyltransferase. *Cancer Discov*, **16**(1): 135-154.

Castellanos G, Camargo-Herrera LV, Rangel N, Jimenez-Tobon GA, Martinez-Aguero M and Rondon-Lagos M (2024). Exploring chromosomal instability and clonal heterogeneity in breast cancer. *Endocr-Relat. Cancer*, **31**(12): e240096.

Castellanos G, Valbuena DS, Perez E, Villegas VE and Rondon-Lagos M (2023). Chromosomal instability as enabling feature and central hallmark of breast cancer. *Breast Cancer-Target*, **15**: 189-211.

ELKasar AO, Hussien FZ, Abdel-Hamied HE, Saleh IG, Mahgoup EM, El-Arabey AA and Abd-Allah AR (2024). Effect of lithium on chemotherapy-induced neutropenia in Egyptian breast cancer patients; A prospective clinical study. *Cancer Chemoth. Pharm.*, **93**(6): 541-554.

Fujii T, Nakazawa Y, Aoki M, Tanabe K, Ogino M, Obayashi S and Shirabe K (2025). Cardioprotective effect of pegfilgrastim on chemotherapy-induced cardiotoxicity in preoperative chemotherapy for breast cancer. *Anticancer Res.*, **45**(4): 1707-1712.

Gaumond SI, Lee KJ, Warp PV, Kamholtz I, Dreifus EM and Jimenez JJ (2025). Parallel toxicities: A comparative analysis of chemotherapy-induced neutropenia and alopecia. *Cancers*, **17**(7): 1163.

Gyawali B, Bohlke K, Dickter JK, Kelkar AH, Knopf KB, Rapoport BL, Roof L, Schott S, Seshadri MR, Shilpakar R, Smith TJ, Trapani D, Woodard AB, Cigler T. WBC Growth Factors: ASCO Guideline Update. J Clin Oncol. (2026) Mar 20;44(9):812-824. doi: 10.1200/JCO-25-02938. Epub 2026 Feb 25. PMID: 41740078.

Hobbs J, Lowe J, Ferdinand A, Shook A, Beck B, Blais D, Borchardt C and Xu B (2023). Efficacy of same-day versus next-day administration of pegfilgrastim for the prevention of chemotherapy-induced febrile neutropenia in breast cancer patients receiving dose-dense doxorubicin and cyclophosphamide: A retrospective multi-site analysis. *J Oncol Pharm Pract*, **29**(8): 1853-1861.

Hosseini M, Feghhi-Najafabadi S and Azad M (2024). A Review on the Impact of Aberrant Methylation in Breast Cancer: Diagnostic, Prognostic, and Therapeutic Approaches. *Iran J. Biotechnol*, **22**(4): e3897.

Huo Q, Chen S, Zhuang J, Quan C, Wang Y and Xie N (2023). SIRT7 downregulation promotes breast cancer metastasis via LAP2α-induced chromosomal instability. *Int J. Biol Sci*, **19**(5): 1528-1542.

Hutajulu SH, Oktariani S, Sunggoro AJ, Bintoro BS, Astari YK, Wiranata JA, Widodo I, Ekowati A, Hardianti MS, Taroeno-Hariadi KW, Kurnianda J and Purwanto I (2023). The occurrence and risk factors of chemotherapy-induced neutropenia in patients with breast cancer not receiving primary G-CSF prophylaxis. *Ecancermedicalscienc*, **17**: 1618.

Joseph A, Joshua JM and Mathews SM (2023). Chemotherapy-induced neutropenia among breast Cancer patients in a tertiary care hospital: Risk and consequences. *J Oncol Pharm Pract*, **29**(3): 529-533.

Kang H, Kim I, Park H, Ahn W, Kim SK and Lee S (2024). Prognostic value of body composition measures in breast cancer patients treated with chemotherapy. *Sci Rep-Uk*, **14**(1): 23309.

Li J, Hubisz MJ, Earlie EM, Duran MA, Hong C, Varela AA, Lettera E, Deyell M, Tavora B, Havel JJ, Phyu SM, Amin AD, Budre K, Kamiya E, Cavallo J, Garris C, Powell S, Reis-Filho JS, Wen H, Bettigole S, Khan AJ, Izar B, Parkes EE, Laughney AM and Bakhoum SF (2023). Non-cell-autonomous cancer progression from chromosomal instability. *Nature*, **620**(7976): 1080-1088.

Liao Y and Cao W (2023). The progress in our understanding of CIN in breast cancer research. *Front Oncol*, **13**: 1067735.

Morecroft R, Logothetics CN, Tarnawsky SP and Davis AA (2024). Chemotherapy-induced neutropenia management in a patient with metastatic breast cancer and Shwachman-Diamond syndrome (SDS): A case report. *Transl Breast Cancer Res*, **5**: 26.

National Comprehensive Cancer Network. (2026). NCCN Guidelines®: Hematopoietic Growth Factors (Version 3.2026). Retrieved from https://www.nccn.org/guidelines/category_3National Comprehensive Cancer Network

Nasir MU, Ghazal TM, Khan MA, Zubair M, Rahman A, Ahmed R, Hamadi HA and Yeun CY (2022). Breast cancer prediction empowered with fine-tuning. *Comput Intel Neurosc*, **2022**: 5918686.

Ong SS, Ho PJ, Khng AJ, Lim EH, Wong FY, Tan BK, Lim SH, Tan EY, Tan S, Tan VKM, Dent R, Tan TJY, Ngeow J, Madhukumar P, Hamzah JLB, Sim Y, Lim GH, Pang JS, Alcantara VS, Chan PMY, Chen JJC, Kuah S, Seah JCM, Buhari SA, Tang SW, Ng CWQ, Li J and Hartman M (2022). Association between breast cancer polygenic risk score and chemotherapy-induced febrile neutropenia: Null results. *Cancers*, **14**(11): 2714.

Payton M, Belmontes B, Hanestad K, Moriguchi J, Chen K, McCarter JD, Chung G, Ninniri MS, Sun J, Manoukian R, Chambers S, Ho S, Kurzeja RJM, Edson KZ, Dahal UP, Wu T, Wannberg S, Beltran PJ, Canon J, Boghossian AS, Rees MG, Ronan MM, Roth JA, Minocherhomji S, Bourbeau MP, Allen JR, Coxon A, Tamayo NA and Hughes PE (2024). Small-molecule inhibition of kinesin KIF18A reveals a mitotic vulnerability enriched in chromosomally unstable cancers. *Nat Cancer*, **5**(1): 66-84.

Salako O, Okunade KS, Adeniji AA, Fagbenro GT and Afolaranmi OJ (2021). Chemotherapy induced neutropenia and febrile neutropenia among breast cancer patients in a tertiary hospital in Nigeria. *Ecancermedicalscienc*, **15**: 1188.

Sandherr M, Schalk E, Heinz WJ, Köhler P, Krause SW, Liss B, Kausche L, Link H, Mellinghoff SC, Schmidt-Hieber M, Schuelper N, Spiekermann K, Sprute R and Seggewiss-Bernhardt R (2026). Evidence-based AGIHO guideline update on prophylaxis of infectious complications with granulocyte-stimulating factors (G-CSF) for the treatment of adult patients with cancer. *Eur J Cancer*., **235**: 116244.

Sohrabi B, Qadbeigi M, Sabouni F and Hamta A (2024). Thymoquinone nanoparticle induces apoptosis and cell migration retardation through modulating of SUMOylation process genes in breast cancer cell line. *Iran J. Biotechnol*, **22**(1): e3676.

Sun H, Li L, Lao I, Li X, Xu B, Cao Y and Jin W (2022). Single-cell RNA sequencing reveals cellular and molecular reprograming landscape of gliomas and lung cancer brain metastases. *Clin Transl Med*, **12**(11): e1101.

Wang Y, Zhao C, Ma P and Jiang D (2023). Outcome and cost-effectiveness analysis of long-acting G-CSF as primary prophylaxis of neutropenia induced by chemotherapy in breast cancer patients, from a retrospective study. *Cancer Control*, **30**: 10732748221140289.

Wuerstlein R, Harbeck N, Grischke E, Forstmeyer D, von Schumann R, Krabisch P, Ludtke-Heckenkamp K, Stefek A, Stoetzer O, Grafe A, Kaltenecker G, Forstbauer H, Augustin D, Schrader I, Tio J, Nitz U, Gluz O, Kates RE and Graeser MK (2021). Protroca: A noninterventional study on prophylactic lipegfilgrastim against chemotherapy-induced neutropenia in nonselected breast cancer patients. *Breast Care*, **16**(1): 50-58.

Zhang H, Qu X, Han L and Di X (2025). DAPL1 identified as a novel prognostic biomarker in breast cancer: Insights from comprehensive in silico analysis. *Iran J. Biotechnol*, **23**(3): e4037.

Zhang Q, Wang Z, Yao W, Wang S, Zhang G, Chen J, Hou Q, Li S, Li H, Ye C, Sun T, Yang H, Chen Z, Wang Z, Liu X, Geng C, Li X, Zhang J, Zheng H and Shao Z (2024). A randomized, multicenter phase III Study of once-per-cycle administration of efbemalenograstim alfa (F-627), a novel long-acting rhG-CSF, for prophylaxis of chemotherapy-induced neutropenia in patients with breast cancer. *BMC Cancer*, **24**(1): 1143.

Zhang Y, Zhang R, Gu W, Jin Y and Ma C (2024). Efficacy and safety of same-day versus next-day administration of PEG-rhG-CSF for the prophylaxis of chemotherapy-induced neutropenia and febrile neutropenia in patients with breast cancer: A retrospective cohort study. *Curr. Med. Res. Opin.*, **40**(12): 2147-2154.

Zhao J, Qiao G, Liang Y, Li J, Hu W, Zuo X, Li J, Zhao C, Zhang X and Du S (2022). Cost-effectiveness analysis of PEG-rhG-CSF as primary prophylaxis to chemotherapy-induced neutropenia in women with breast cancer in China: Results based on real-world data. *Front Pharmacol*, **12**: 754366.